Photosynth Res (2010) 104:211–219
DOI 10.1007/s11120-010-9541-0

REGULAR PAPER

The lamellar spacing in self-assembling bacteriochlorophyll aggregates is proportional to the length of the esterifying alcohol

Jakub Pšenčík · Mika Torkkeli · Anita Zupčanová · František Vácha · Ritva E. Serimaa · Roman Tuma

Received: 9 October 2009 / Accepted: 24 February 2010 / Published online: 20 March 2010

Abstract Chlorosomes from green photosynthetic bacteria are large photosynthetic antennae containing self-assembling aggregates of bacteriochlorophyll *c*, *d*, or *e*. The pigments within chlorosomes are organized in curved lamellar structures. Aggregates with similar optical properties can be prepared in vitro, both in polar as well as non-polar solvents. In order to gain insight into their structure we examined hexane-induced aggregates of purified bacteriochlorophyll *c* by X-ray scattering. The bacteriochlorophyll *c* aggregates exhibit scattering features that are virtually identical to those of native chlorosomes demonstrating that the self-assembly of these pigments is fully encoded in their chemical structure. Thus, the hexane-induced aggregates constitute an excellent model to study the effects of chemical structure on assembly. Using bacteriochlorophyllides transesterified with different alcohols we have established a linear relationship between the esterifying alcohol length and the lamellar spacing. The results provide a structural basis for lamellar spacing variability observed for native chlorosomes from different species. A plausible physiological role of this variability is discussed. The X-ray scattering also confirmed the assignments of peaks, which arise from the crystalline baseplate in the native chlorosomes.

Keywords Green photosynthetic bacteria · Chlorosome · Bacteriochlorophyll · Aggregate · Bacteriochlorophyllide · X-ray scattering

J. Pšenčík
Department of Chemical Physics and Optics,
Faculty of Mathematics and Physics, Charles University,
Prague, Czech Republic

J. Pšenčík (✉) · A. Zupčanová · F. Vácha
Institute of Physical Biology, University of South Bohemia,
Nové Hrady, Czech Republic
e-mail: psencik@karlov.mff.cuni.cz

M. Torkkeli · R. E. Serimaa
Department of Physics, University of Helsinki, Helsinki, Finland

A. Zupčanová · F. Vácha
Biology Centre, Academy of Sciences of the Czech Republic,
České Budějovice, Czech Republic

R. Tuma
The Astbury Centre for Structural Molecular Biology,
University of Leeds, Leeds, UK

Introduction

Green photosynthetic bacteria exhibit large light-harvesting complexes called chlorosomes, which are ellipsoidal particles with typical dimensions of 150 × 50 × 20 nm. Chlorosomes are composed of self-assembled bacteriochlorophylls (BChl) *c*, *d*, or *e* (Blankenship and Matsuura 2003; Frigaard and Bryant 2006). In addition, chlorosomes contain BChl *a*, carotenoids, quinones, and lipids. BChl *a* is located in the crystalline baseplate connecting the chlorosome to the cytoplasmic membrane (via FMO protein layer in green sulfur bacteria). Proteins are located only in the baseplate and an envelope of the chlorosome (Chung and Bryant 1996; Vassilieva et al. 2002). A lamellar model for arrangement of BChl molecules within chlorosomes was proposed on the basis of X-ray scattering and electron cryomicroscopy (cryo-EM) (Psencik et al. 2004). In this model, BChl aggregates form lamellar structures with lamellar spacing between 2 and 4 nm, depending on the main BChl type. Interdigitated esterifying alcohols hold the lamellar layers together and provide a hydrophobic environment for accumulation of carotenoids

and quinones (Psencik et al. 2006). In green sulfur bacterium *Chlorobaculum* (*Cba.*) *tepidum* (formerly known as *Chlorobium* (*Chl.*) *tepidum*) the lamellar system often remains parallel to the main axis of the chlorosome, while it exhibits considerable curvature in the two perpendicular directions. This curvature was initially interpreted as being due to general undulations (Psencik et al. 2004). Later Oostergetel et al. (2007) obtained end-on cryo-EM projections of the chlorosomes from *Cba. tepidum* which enabled direct visualization of the curved lamellar structures, including lamellar tubules as well as undulations. Cryo-EM and nuclear magnetic resonance experiments on chlorosomes from a *Cba. tepidum* mutant containing single BChl *d* homolog led recently to a proposal that BChl aggregates form concentric nanotubes with BChls arranged into helical spirals (Ganapathy et al. 2009). Lamellar arrangement was also observed in the brown-colored green sulfur bacteria, belonging to the same Chlorobi phylum as *Cba. tepidum*, but containing BChl *e* as the main pigment. In these chlorosomes bulk of the aggregates is composed of smaller lamellar domains, which exhibit random relative orientations, and parallel lamellar system is only found in the proximity of the baseplate (Psencik et al. 2006). Recently, the presence of lamellar aggregates was demonstrated in BChl *c* containing chlorosomes from *Chloroflexus* (*Cfl.*) *aurantiacus* (Psencik et al. 2009), a member of a different phylum than the previously studied Chlorobi species. This finding suggests that the lamellar organization is universal among all types of chlorosomes and perhaps an intrinsic property of the chlorosomal bacteriochlorophylls, although the higher-order structure may differ between species and reflect subtle variations in the composition. In addition, comparison of chlorosomes from different species suggests that the lamellar spacing is approximately proportional to the chain length of the esterifying alcohols. Larger spacing also correlates with an increasing number of lipophilic components (i.e., carotenoids and quinones) that partition with the esterifying alcohols into the apolar space of the lamellar system (Psencik et al. 2006).

Self-assembling aggregates with similar properties to those in chlorosome can also be prepared in vitro (for a review see Balaban et al. 2005; Miyatake and Tamiaki 2005). Studies proved that an addition of non-polar compound (lipid, carotenoid, quinone) is necessary for aggregation of BChl *c* from green sulfur bacteria in aqueous solutions (Hirota et al. 1992; Klinger et al. 2004; Alster et al. 2008). The hydrophobic effect stabilizes the interactions between esterifying alcohols and other lipophilic components and constitutes the driving force for self-assembly under these conditions. Aggregates can also be prepared in non-polar organic solvents such as hexane (Smith et al. 1983). In this case the assembly is most likely driven by the hydrophilic interaction between the polar groups on chlorin rings (Zupcanova et al. 2008). BChl *c* aggregates from hexane exhibit very similar nuclear magnetic resonance pattern as chlorosomes (van Rossum et al. 1998) suggesting that the short-range arrangement is similar in both cases; however, it is not clear whether also the long-range arrangement (i.e., lamellar organization) is the same as in chlorosomes. This question is addressed in this study, showing that the hexane-induced BChl *c* aggregates exhibit a structure remarkably similar to that found in chlorosomes. The main objective of this study, however, was to further explore the structural role of the esterifying alcohol in the lamellar arrangement. Using bacteriochlorophyllides exhibiting increasing length of the esterifying alcohol we show that the lamellar spacing is proportional to this length.

Materials and methods

Cells of *Cba. tepidum* were grown in modified Pfenning's medium (Wahlund et al. 1991) for 3 days at 48°C under constant illumination from a 60-W tungsten lamp. Pigments were extracted from whole cells using a mixture of acetone and methanol (7:2, vol/vol). BChl *c* was isolated from the extract by means of reverse-phase HPLC as described in (Klinger et al. 2004). The four main C8 and C12 homologs of BChl *c* esterified with farnesyl at $C17^3$ (Fig. 1) were combined. 8-ethyl-12-ethyl BChl *c* ([E,E]BChl c_F) and 8-propyl-12-ethyl BChl *c* ([P,E]BChl c_F) were the two most abundant homologs used in this study, accounting for 60 and 30% of the total content, respectively. Pigments were dried and stored at −20°C. BChl *c* aggregates in hexane were prepared by dissolving purified BChl *c* in dichloromethane (concentration ~1 mM). Aggregates were formed immediately upon addition of at least 10-fold excess of neat hexane followed by vigorous mixing. The resulting aggregates were sedimented and slowly dried with nitrogen at room temperature to prepare sample for powder X-ray scattering. Bacteriochlorophyllide *c* (BChlide *c*) derivatives esterified with methyl, butyl, and octyl at the $C17^3$ position (Fig. 1) were prepared from BChl *c* by transesterification under KOH alkaline conditions as described earlier (Zupcanova et al. 2008). Aggregates from all transesterified BChlides *c* in hexane were prepared in the same way as hexane-induced aggregates from BChl *c*.

The small and medium angle X-ray scattering (SAXS and MAXS) measurements were performed as described earlier (Psencik et al. 2004) using a setup comprising sealed Cu fine-focus X-ray tube, Montel Optics by Incoatec GmbH and HI-STAR 2-D multi-wire proportional counter as a detector. Sample to detector distances were 50 and 18 cm, respectively. The wide-angle X-ray scattering

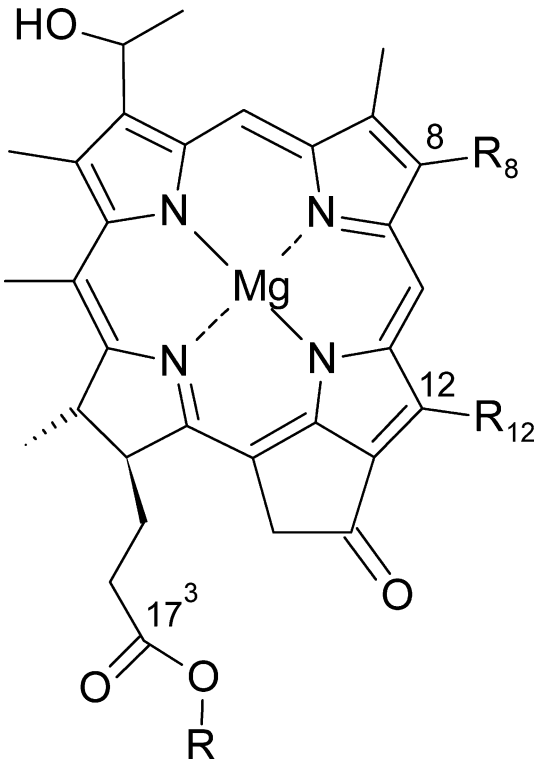

Fig. 1 Molecular structure of BChlide *c*. R stands for the alkyl group of the esterifying alcohol. In this study, BChlides esterified with methyl, butyl, and octyl were used and compared with BChl *c* esterified with farnesyl. Substituents R_8 can be mainly ethyl, propyl, or isobutyl, R_{12} can be methyl or ethyl

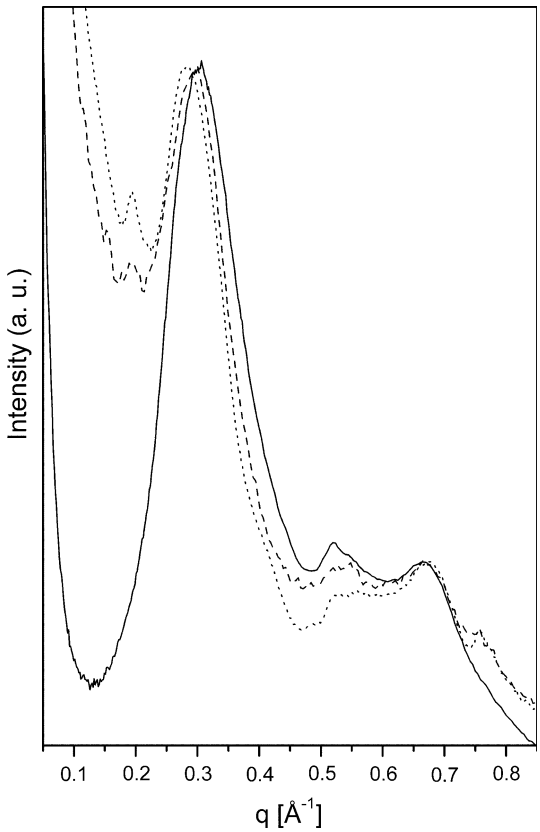

Fig. 2 X-ray scattering curve from dried BChl *c* aggregate (*solid line*) compared with scattering curves from two different *Cba. tepidum* chlorosome samples (*dotted line*, data from (Psencik et al. 2004) and dashed line, data from (Ikonen et al. 2007)) to illustrate the natural variability of the scattering patterns

(WAXS) was measured with an in-house X-ray system utilizing Rigaku rotating anode source (0.3 mm × 0.3 mm Cu target), focusing optics based on a curved Cu-plated mirror and a curved asymmetric Si(111) monochromator crystal and MAR345 image plate detector placed on the focal point. The dried samples were cleaved into thin flakes which were subsequently mounted and exposed to X-rays along the cleavage plane. Scattering anisotropy was measured by directing the incident X-ray beam along the surface of the dried thin flakes (ca. 1 × 2 mm). The anisotropic scattering patterns were integrated sector-by-sector to preserve the orientation information as shown in Fig. 3.

Results

BChl *c* aggregates in hexane

Figure 2 compares X-ray scattering measurements on BChl *c* aggregates from hexane with scattering curves of BChl *c* containing chlorosomes from *Cba. tepidum*. The scattering curves from two different chlorosome preparations illustrate the natural variability of the scattering pattern. The scattering of BChl *c* aggregates from hexane is very similar to the scattering from chlorosomes. Each of the three peaks (∼0.3, 0.52, and 0.66 1/Å) observed for the dried aggregates have a corresponding peak in the chlorosomal diffraction pattern. The agreement between their relative intensities and widths is also excellent. This result thus confirms that the three peaks at *q* values of ∼0.3, 0.52, and 0.66 1/Å observed in the scattering from native chlorosomes originate solely from BChl *c* aggregates, as previously proposed.

In native chlorosomes the q ∼ 0.3 1/Å peak was assigned to the lamellar spacing on the basis of cryo-EM and other evidence (Psencik et al. 2004). The X-ray data presented here show that the hexane-induced aggregates are also organized into lamellar structures. The lamellar spacing of the hexane-induced aggregate (20.7 Å) is somewhat smaller than that observed for wild-type *Cba. tepidum* chlorosomes in Fig. 2 (∼21–22 Å). This most likely reflects changes to lamellar packing due to carotenoids, which are absent from the hexane-induced aggregates (see "Discussion" section and Psencik et al. (2006)).

While the position of the lamellar peak is somewhat variable, the positions of the two remaining peaks, i.e., at 0.52–0.54 1/Å and 0.66–0.68 1/Å, respectively, exhibit much less variability in chlorosomes and also in aggregates. We propose that these two peaks reflect the arrangement of the BChl *c* within individual lamellar layers and reflect distances within and between pigment stacks. Although it is not possible to construct a unique lattice from this data alone the observed Bragg distances are compatible with a dimer in the asymmetric unit as previously proposed (Psencik et al. 2004).

Scattering from native chlorosomes exhibits two additional peaks when compared to that from the hexane-induced aggregate. These two peaks are less intense, but significantly sharper compared to the peaks attributed to BChl *c*. In addition, their position at 0.195 1/Å (32.2 Å spacing) and 0.76 1/Å (spacing 8.2 Å) does not vary between different wild-type chlorosome preparations. These peaks were affected for carotenoids deficient *Cba. tepidum* mutants that exhibit defects in chlorosome morphogenesis, and it was argued that these changes reflect structural rearrangements of the baseplate (Ikonen et al. 2007). In addition, both peaks disappeared during treatment of the chlorosomes with hexanol, and their disappearance correlated well with an overall change of the chlorosome shape from ellipsoidal to a round one, which was attributed to the destruction of the baseplate (Arellano et al. 2008). Based on such indirect evidence, these two peaks were suggested to arise from the chlorosome crystalline baseplate. Absence of the two peaks from the scattering pattern of hexane-induced aggregates is consistent with this interpretation.

It is interesting to note that X-ray scattering patterns of both chlorosomes and BChl *c* aggregates from hexane exhibit a significant and similar anisotropy. Figure 3 shows the orientation of the four X-ray scattering reflections measured from a thin flake of a dried chlorosome sample. Two reflections have dominant contribution in the direction normal to the plane of the flake while the other two are parallel. The lamellar peak reflection (peak I in the Fig. 3) contributes to scattering in the normal direction reflecting the typical lamellar morphology. The ~0.66 1/Å peak (peak III) exhibits anisotropy similar to the lamellar peak despite not being directly related (e.g., second order). Assuming that the chlorosomes are oriented within the flake with their long axis parallel to the surface the data suggest that the lattice vector **c** (i.e., the lamellar spacing; lattice vectors defined in (Psencik et al. 2004), see also Fig. 3 here) is oriented perpendicular to the long axis of the chlorosome while **b** (peak II) and the 0.76 1/Å baseplate spacing (peak IV) are oriented along the long axis of the chlorosome. Lattice vector **a** (peak III) has the dominant contribution in the direction perpendicular to the long axis

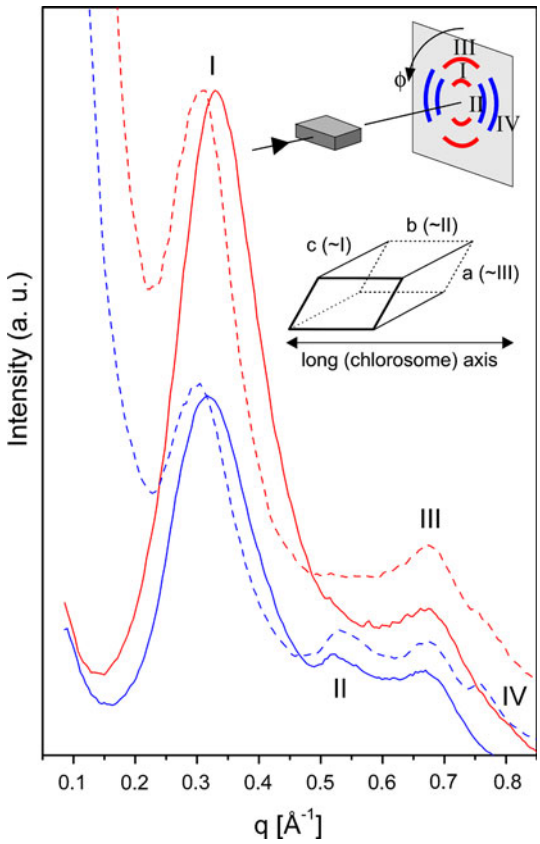

Fig. 3 Anisotropic X-ray scattering curves from a dried BChl *c* aggregate (*solid line*) and *Cba. tepidum* chlorosome (*dotted line*). MAXS intensities in the direction normal (*red line*) and parallel (*blue line*) to the flake, integrated over 60° sectors in the detector plane (angle ϕ). The inset at the top illustrates the sample-detector configuration used for data acquisition. The inset below shows the orientation of the unit cell with respect to the long axis of the chlorosome or the aggregate flake, respectively. The lattice constant **c** (lamellar spacing, see also Fig. 6) is perpendicular to the long axis

of the chlorosome. Unfortunately, the 0.195 1/Å baseplate peak was not well resolved in the anisotropic measurements, presumably because of its position on the sharply decaying baseline. After subtraction of the baseline (not shown) the peak was resolved in the parallel scattering indicating that the main baseplate spacing (32.2 Å) is oriented along the long axis of the chlorosome, in agreement with the recent direct cryo-EM observation for *Cfl. aurantiacus* (Psencik et al. 2009).

BChlide *c* aggregates in hexane

Given the proposed aggregate structure, with the esterifying alcohols filling the space between lamellar layers, the lamellar spacing shall be proportional to the length of the esterifying alcohol (Fig. 6). In order to examine this relationship we prepared a series of BChlides *c* differing in the length of the esterifying alcohol (methyl, butyl, and octyl).

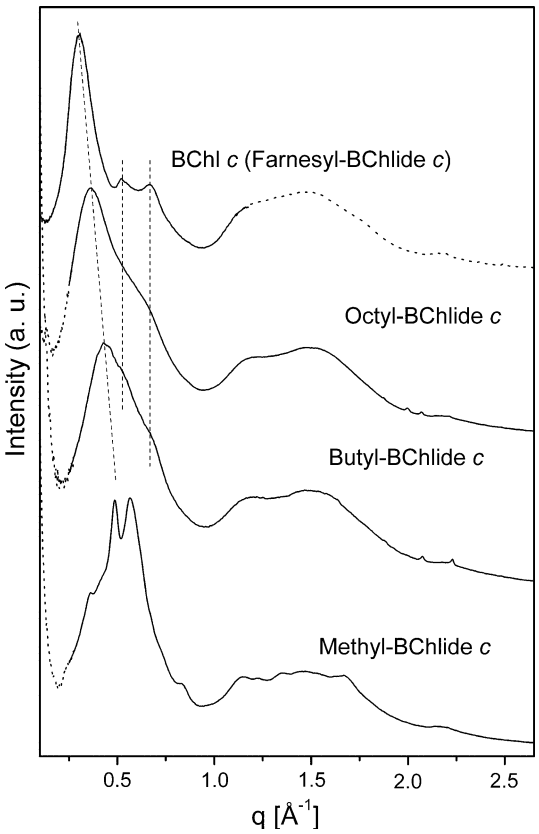

Fig. 4 X-ray scattering curves of aggregates prepared in hexane from BChl *c* esterified with farnesyl and several BChlides *c*. Data for BChl *c* are combined from MAXS and WAXS measurements; data from BChlides are combined form SAXS and WAXS measurements. The several sharp peaks observed in the wide-angle region are most likely from a residual dried potassium hydroxide, which was used during the BChlides preparation

All three compounds formed aggregates in hexane which in turn exhibited optical spectra almost identical to those obtained for aggregates from BChl *c* esterified by farnesyl, as shown previously (Zupcanova et al. 2008). Figure 4 compares X-ray scattering patterns of the BChlide aggregates with that of BChl *c* esterified with farnesyl. Methyl-BChlide *c* diffraction is dominated by two peaks at 0.49 and 0.57 1/Å. Together with two weaker peaks at 0.36 and 0.83 1/Å the scattering pattern does not resemble that of BChl *c* aggregates. This compound may adopt a polycrystalline form distinct from the lamellar aggregates. The two lower angle peaks were found at nearly identical positions (at 0.35 and 0.48 1/Å, respectively) in previous study of methyl-BChlide *c* aggregates (note that the higher angle peaks were outside the q range used in the study, $q < 0.55$ 1/Å) (Umetsu et al. 1999). In contrast to methyl-BChlide *c*, both butyl and octyl derivatives yield patterns similar to that of BChl *c* with the exception of the lamellar peak which progressively shifted from ~0.3 1/Å for farnesyl to 0.36 1/Å (lamellar spacing of 17.5 Å) for octyl, and finally to 0.44 1/Å (lamellar spacing of 14.3 Å) for the butyl substitution. Other peaks reflecting the order within the lamellar layers remained at the same positions, indicating that pigment arrangement within stacks was conserved. This is consistent with their chlorosome-like visible spectra. Consequently, lamellar spacing does not influence the short-range order of assembled pigments and their spectral properties. The wide-angle patterns ($q > 1$ 1/Å) were very similar for all pigments, further confirming their similar short-range packing.

Discussion

Comparison of X-ray scattering profiles obtained from chlorosomes of *Cba. tepidum* and BChl *c* aggregates from hexane confirms that the peaks at *q* values of ~0.3, 0.52, and 0.66 1/Å originate from BChl *c* aggregates. The data also demonstrate that the same lamellar structures are formed, including the extent of disorder, no matter whether the aggregates are assembled in cells into native chlorosomes or in vitro in a non-polar organic solvent. Thus, the self-organization is remarkably robust and encoded in the chemical structure of the pigment alone. Lamellar structures are formed also by aggregates of butyl-BChlide *c* and octyl-BChlide *c* but not by methyl-BChlide *c*. The fact that the X-ray scattering from methyl-BChlide *c* aggregates differs significantly from the other derivatives is consistent with an important role of the esterifying alcohol length in the formation of lamellar structures (Zupcanova et al. 2008).

In this study, a natural mixture of BChl *c* homologs as found in native chlorosomes was used for hexane-induced assembly. Similar lamellar structures were obtained for synthetic BChl *c* analogs, and it was noted that racemic mixture supported assembly more readily than isolated epimers alone (Balaban 2005). A similar conclusion has been drawn also for BChls in native chlorosomes (Steensgaard et al. 2000). This may explain why no X-ray scattering from a hexane-induced BChl *c* aggregate had been observed when a single BChl *c* homolog *R*[E,E]BChl c_F was used (Umetsu et al. 1999). In the same study (Umetsu et al. 1999) X-ray scattering from methyl-BChlide *c*, which was a mixture of all naturally occurring homologs, yielded very similar results to those presented here. On the other hand, similar X-ray scattering patterns were obtained for dichloromethane-induced aggregates of either a natural mixture of BChl *c* homologs used in this study (unpublished data) or a single *R*[E,E]BChl c_F homolog (Umetsu et al. 1999). The presence of well-ordered aggregates in the mutant producing a single BChl *d* homolog (Oostergetel et al. 2007; Ganapathy et al. 2009) also suggests that the roles of various homologs and epimers in aggregation are far from being understood.

The 0.76 1/Å diffraction was originally assigned to a 110 reflection from the proposed monoclinic lattice of BChl *c* aggregates (Psencik et al. 2004). The absence of this and another chlorosome peak ($q = 0.195$ 1/Å) from the diffraction of the hexane-induced aggregate demonstrates that these two peaks must originate from a different periodic structure within the chlorosome, most probably the crystalline baseplate. This interpretation is supported by the fact that these peaks are diminished in intensity when the integrity of the baseplate is affected, e.g., as a consequence of mutagenesis (Ikonen et al. 2007) or hexanol treatment (Arellano et al. 2008). In addition, these two peaks are significantly sharper than those originating from BChl aggregates. Finally, the Bragg spacing corresponding to 0.195 1/Å peak (32.2 Å) and its orientation along the long axis of the chlorosome fits very well with the baseplate spacing (33 Å) and orientation observed in chlorosomes from *Cfl. aurantiacus* by cryo-EM (Psencik et al. 2009). The 0.76 1/Å peak (8.2 Å spacing) most likely reflects packing order within the baseplate, perhaps spacing between α-helices within a dimer of the CsmA protein (Pedersen et al. 2008; Psencik et al. 2009).

The lamellar spacing, observed here for the BChl *c* derivatives, when plotted as a function of the length of the esterifying alcohol, increases approximately linearly (Fig. 5). Thus, the lamellar spacing is proportional to the length of the esterifying alcohol, as illustrated schematically in Fig. 6. Absorption spectra of aggregates from all studied BChlides and BChl *c* in hexane are very similar, including position of the Q_y band absorption maxima at ~745 nm (Zupcanova et al. 2008). The Q_y band of monomeric BChl *c* exhibits a peak at around 670 nm, and the red shift of the Q_y band in aggregates, observed for both the hexane-induced aggregates and native chlorosomes, is caused by excitonic interactions between the transition dipole moments of the monomers. The data presented here demonstrate that aggregates exhibiting the same red shift differ in their lamellar spacing. This means that only interactions within the same lamellar layer contribute significantly to the excitonic coupling, even for a thickness of ~1.5 nm of butyl-BChlide (absorption spectra of methyl-BChlide are also very similar, but for this compound we do not have a clear evidence that it forms lamellar aggregates). As a consequence, only a single pigment layer should be sufficient for excitonic calculations of the spectral properties of BChl aggregates in chlorosomes. It is interesting to note that the excitonic interactions within lamellar layers can be reversibly abolished by treatment with hexanol without disrupting the lamellar order, at least in native chlorosomes (Arellano et al. 2008).

In addition to data obtained for aggregates in vitro, Fig. 5 also illustrates how the lamellar spacing varies upon change of the esterifying alcohol length and carotenoid content in chlorosomes from different species. The data for chlorosomes deviate from the extrapolated linear dependence, being systematically larger than the predicted value. However, the data presented in Fig. 5 also suggest that this deviation is caused mainly by the additional amount of carotenoids, and probably also quinones, which are not present in the in vitro aggregates. Both carotenoids and quinones were shown to co-habit the hydrophobic space between the lamellar layers with esterifying alcohols. When majority of these hydrophobic molecules are washed out from the chlorosome by hexane treatment the spacing decreases to a value close to the extrapolated linear relationship. In Fig. 5, this is illustrated by a spacing decreased from 27.3 to 22.4 Å observed for chlorosomes from *Chl. phaeovibrioides* (Psencik et al. 2006). Similarly, spacings close to the predicted value were observed for *Cba. tepidum* chlorosomes, which harbor only small amount of carotenoids.

While the spacing clearly increases with the amount of carotenoids, no quantitative relationship can be derived based on present data. This is because the dependence is complicated by the presence of quinones which will certainly contribute to the lamellar spacing. In addition, a certain carotenoid fraction is present in the baseplate, and thus does not contribute to the spacing. Finally,

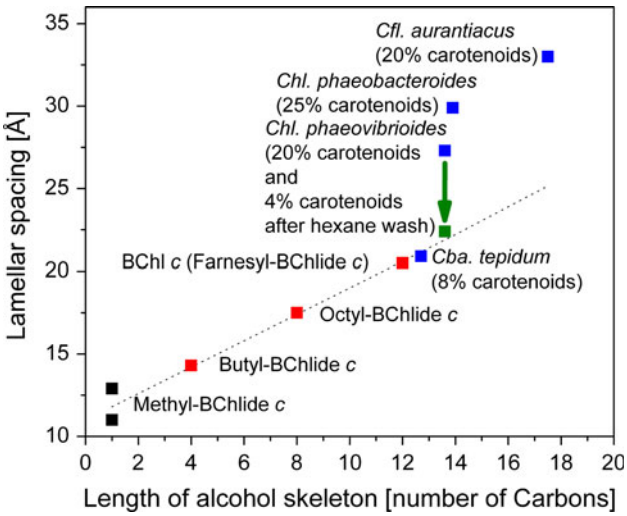

Fig. 5 Scaling of lamellar spacing with the chain length. Spacings corresponding to the two main peaks observed for methyl-BChlide *c* are shown (*black*). The data points obtained for hexane-induced aggregates of other BChlides and farnesyl-BChl *c* (*red*) were used to produce the linear fit (*dotted*). Blue data points correspond to the lamellar spacing in native chlorosomes (data from Psencik et al. 2004, 2006, 2009). The *green arrow* depicts the change in lamellar spacing upon carotenoids and quinones removal by a hexane wash (Psencik et al. 2006). The lengths of the esterifying alcohols are based on the HPLC analysis of the same chlorosomes from green sulfur bacteria (Psencik et al. 2006) and *Cfl. aurantiacus* (Psencik et al. 2009), which were used in the X-ray experiments. Average lengths of the carbon skeletons of alcohols were calculated ignoring their methyl substituents

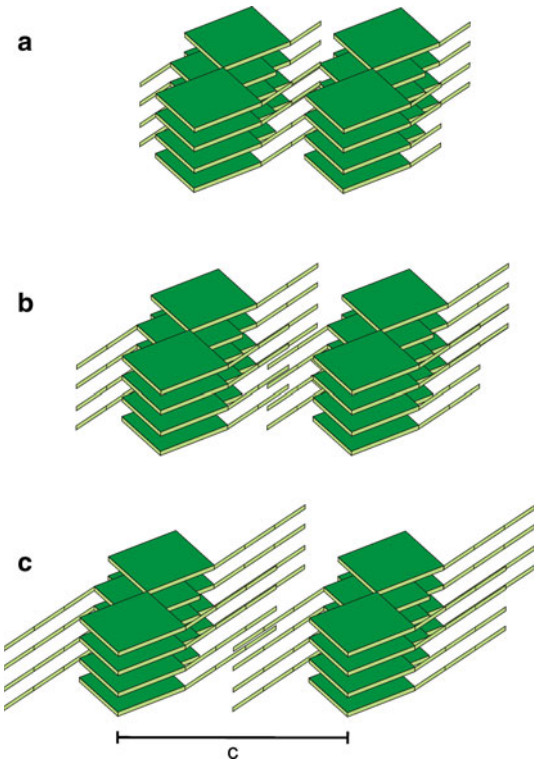

Fig. 6 Scheme illustrating the proposed scaling of lamellar spacing with the esterifying alcohol tail length. Polar chlorin rings of BChl molecules are depicted as green plates and the apolar alcohol tails as sticks. In this scheme the lamellar curvature is not apparent

chlorosomes from different species contain different carotenoids, which may occupy more or less lamellar space due to their various sizes, conformations, and possibly also have distinct interactions with BChls. This is illustrated by structural characterization of *Cba. tepidum* mutants that accumulate different carotenoid variants (Ikonen et al. 2007). The largest spacing (23.7 Å) was observed for a mutant harboring phytoene in the 15-*cis* conformation, a carotenoid analog that is likely to occupy larger excluded volume within the lamellae than the carotenoids normally present in the wild-type chlorosome. In general, the lamellar spacing is primarily determined by the length of esterifying alcohols and may be further modulated by the excluded volume of carotenoids and quinones.

Now, a question may arise whether the observed correlations between the average length of the esterifying alcohols and the lamellar spacing have any physiological significance. The smallest lamellar spacing (~2 nm) and carotenoid content (carotenoid/BChl molar ratio of ~0.1:1) was found in *Cba. tepidum,* which lives anaerobically under moderate light conditions (Wahlund et al. 1991; Castenholz and Pierson 1995) and therefore can survive without extra light-harvesting capability or protection by carotenoids. On the other hand, BChl *e* containing brown-colored species of green sulfur bacteria often live in deeper water layers under very low light conditions. Due to the light scattering and absorption of the water column and phytoplankton, mainly light in the spectral region between 500 and 600 nm reaches their habitat (Vila and Abella 1994). Bacteria adapt to these conditions by an unusual splitting of the Soret absorption band of the aggregated BChl *e* (Cox et al. 1998; Arellano et al. 2000) and by formation of small domains of lamellar aggregates with different orientations, presumably to capture photons with different polarizations (Psencik et al. 2006). In addition, chlorosomes of brown-colored bacteria contain large amounts of carotenoids, which are able to increase absorption in a broad range around 500 nm. Brown-colored species exhibit on the average longer esterifying alcohols and consequently larger lamellar spacing compared to *Cba. tepidum.* This enables them to accommodate the additional carotenoids. The important role of carotenoids for light-harvesting was demonstrated by observation of efficient (60–70%) and fast energy transfer (transfer time faster than 100 fs) from the short-lived carotenoid S_2 state to BChls in chlorosomes from brown-colored green sulfur bacterium *Chl. phaeobacteroides* (Psencik et al. 2002).

In contrast to green sulfur bacteria, *Cfl. aurantiacus* is a facultative aerobic bacterium and therefore protection of photosynthetic apparatus against oxidative damage is required. Carotenoids are known, apart from their light harvesting function, to provide photo-protection to the photosynthetic apparatus. Indeed, a considerably enhanced carotenoid biosynthesis was observed for *Cfl. aurantiacus* under intense irradiation (Schmidt et al. 1980; Larsen et al. 1994; Ma et al. 1996). This suggests that under these conditions carotenoids have a protective rather than light-harvesting function. As a result, the carotenoid/BChl *c* molar ratio can be as high as 0.45:1 in *Cfl. aurantiacus* (Schmidt et al. 1980), which is one of the highest ratios among all green bacteria. As for the brown-colored green sulfur bacteria, large lamellar spacing is required in this case to accommodate the additional carotenoids. Therefore, it is not surprising that BChl *c* in *Cfl. aurantiacus* is esterified with the longest esterifying alcohols (dominating alcohol is octadecanol) and consequently exhibits the largest lamellar spacing (~3.3 nm) among all green bacteria studied. Thus, the data presented here suggest that the observed correlation between the length of the esterifying alcohol and the lamellar spacing is a mechanism used by various bacteria to accommodate larger amounts of carotenoids either for light harvesting or photo-protection.

Another consequence of the larger lamellar spacing is an increased observed disorder within the BChl aggregate. This additional disorder is probably the main reason why the two peaks assigned to the lattice within the lamellar

layers (0.52 and 0.66 1/Å) were not observed for chlorosomes from BChl *e* containing green sulfur bacteria and from *Cfl. aurantiacus*, i.e., the species containing BChls with longer esterifying alcohols.

The three main scattering peaks of BChl *c* yielded a unit cell for the aggregate arrangement and the corresponding cell dimensions are compatible with a dimer of BChl *c* molecules in the asymmetric unit (Psencik et al. 2004). Self-assembly experiments with BChl *c* and BChlide *c* molecules revealed an important role of the esterifying alcohols, and favor structural models where alcohol tails extend to both sides of the lamellar layer (Klinger et al. 2004; Zupcanova et al. 2008). Such an arrangement facilitates the hydrophobic interaction between esterifying alcohols from the neighboring layers and provides plausible explanation for the formation of lamellae. Two previously proposed models fulfill these two requirements. One of them invokes an antiparallel piggyback dimer as the building block (Nozawa et al. 1994; Egawa et al. 2007) while the other proposes a unit cell containing two parallel monomers with alternating *syn* and *anti* configuration (Ganapathy et al. 2009). In that study, *syn* and *anti* refers to the orientation of the OH ligation of adjacent BChls with respect to the farnesyl tail. The lattice dimensions of both models are in principle compatible with the X-ray data presented here. A schematic illustration of the arrangement of aggregates shown in Fig. 6 is thus valid for both models. The anisotropic X-ray data allowed to determine the preferred orientation of the ordered lamellar system and its unit cell within the chlorosome. As expected, the lamellar spacing (lattice vector **c**) is oriented normal to the long axis of the chlorosome, lattice vector **a** nearly normally. Axis **b** is parallel to the main axis of the chlorosome. The same conclusion can be drawn also for in vitro aggregates. In this case the role of long axis of the chlorosome is replaced by any axis parallel to the sample flake. The X-ray data are consistent with a presence of curved lamellae and open, partially formed multilayered cylinders as shown by cryo-EM (Oostergetel et al. 2007). The lattice from (Psencik et al. 2004) ($\mathbf{a} = 9.6$ Å, $\mathbf{b} = 12.0$ Å, $\mathbf{c} = \sim 20$ Å) and its orientation in respect to the long axis of the chlorosome proposed here is similar to the model shown in Fig. 5c of Ganapathy et al. (2009) (note the different lattice constant designations, here we have $\mathbf{a} < \mathbf{b} < \mathbf{c}$ while Ganapathy et al. (2009) uses $\mathbf{b} = 9.8$ Å $< \mathbf{a} = 12.5$ Å).

In summary, the pigment arrangement of BChl *c* in hexane-induced aggregates is virtually identical to that seen in native chlorosomes, including the lamellar spacing, which scales with the length of esterifying alcohols. The scalable spacing enables native chlorosomes to accommodate variable amounts of carotenoids in response to changing growth conditions. Thus, the BChl molecule is a versatile, self-assembling building block.

Acknowledgments This study was supported by Czech Ministry of Education, Youth and Sports (projects MSM0021620835, MSM6007 665808, AV0Z50510513) and Czech Science Foundation (206/09/0375); R.T. was supported by Academy of Finland (project 118462) and The University of Leeds.

References

Alster J, Zupcanova A, Vacha F, Psencik J (2008) Effect of quinones on formation and properties of bacteriochlorophyll *c* aggregates. Photosynth Res 95:183–189

Arellano JB, Melo TB, Borrego CM, Garcia-Gil J, Naqvi KR (2000) Nanosecond laser photolysis studies of chlorosomes and artificial aggregates containing bacteriochlorophyll *e*: evidence for the proximity of carotenoids and bacteriochlorophyll *a* in chlorosomes from *Chlorobium phaeobacteroides* strain CL1401. Photochem Photobiol 72:669–675

Arellano JB, Torkkeli M, Tuma R, Laurinmaki P, Melo TB, Ikonen TP, Butcher SJ, Serimaa RE, Psencik J (2008) Hexanol-induced order-disorder transitions in lamellar self-assembling aggregates of bacteriochlorophyll *c* in *Chlorobium tepidum* chlorosomes. Langmuir 24:2035–2041

Balaban TS (2005) Tailoring porphyrins and chlorins for self-assembly in biomimetic artificial antenna systems. Acc Chem Res 38:612–623

Balaban TS, Tamiaki H, Holzwarth AR (2005) Chlorins programmed for self-assembly. Top Curr Chem 258:1–38

Blankenship RE, Matsuura K (2003) Antenna complexes from green photosynthetic bacteria. In: Green BR, Parson WW (eds) Light-harvesting antennas in photosynthesis, pp 195–217. Kluwer Academic Publishers, Dordrecht

Castenholz RW, Pierson BK (1995) Ecology of thermophilic anoxygenic phototrophs. In: Blankenship RE, Madigan MT, Bauer CE (eds) Anoxygenic photosynthetic bacteria, pp 87–103. Kluwer Academic Publisher, Dordrecht, The Netherlands

Chung S, Bryant DA (1996) Characterization of the csmD and csmE genes from *Chlorobium tepidum*. The CsmA, CsmC, CsmD, and CsmE proteins are components of the chlorosome envelope. Photosynth Res 50:41–59

Cox RP, Miller M, Aschenbrucker J, Ma YZ, Gillbro T (1998) The role of bacteriochlorophyll e and carotenoids in light harvesting in brown-colored green sulfur bacteria. In: Garab G (ed) Photosynthesis: mechanisms and effects, vol 1. Kluwer Academic Publishers, Dordrecht, pp 149–152

Egawa A, Fujiwara T, Mizoguchi T, Kakitani Y, Koyama Y, Akutsu H (2007) Structure of the light-harvesting bacteriochlorophyll *c* assembly in chlorosomes from *Chlorobium limicola* determined by solid-state NMR. Proc Natl Acad Sci 104:790–795

Frigaard NU, Bryant DA (2006) Chlorosomes: antenna organelles in photosynthetic green bacteria. In: Shively JM (ed) Complex intracellular structures in prokaryotes (series: Microbiology Monographs, vol 2. Springer, Berlin, pp 79–114

Ganapathy S, Oostergetel GT, Wawrzyniak PK, Reus M, Chew AGM, Buda F, Boekema EJ, Bryant DA, Holzwarth AR, de Groot HJM (2009) Alternating syn-anti bacteriochlorophylls form concentric helical nanotubes in chlorosomes. Proc Natl Acad Sci USA 106:8525–8530

Hirota M, Moriyama T, Shimada K, Miller M, Olson JM, Matsuura K (1992) High degree of organization of bacteriochlorophyll *c* in chlorosome-like aggregates spontaneously assembled in aqueous solution. Biochim Biophys Acta 1099:271–274

Ikonen TP, Li H, Psencik J, Laurinmaki PA, Butcher SJ, Frigaard NU, Serimaa RE, Bryant DA, Tuma R (2007) X-ray scattering and electron cryomicroscopy study on the effect of carotenoid

biosynthesis to the structure of *Chlorobium tepidum* chlorosomes. Biophys J 93:620–628

Klinger P, Arellano JB, Vacha FE, Hala J, Psencik J (2004) Effect of carotenoids and monogalactosyl diglyceride on bacteriochlorophyll *c* aggregates in aqueous buffer: Implications for the self-assembly of chlorosomes. Photochem Photobiol 80:572–578

Larsen KL, Cox RP, Miller M (1994) Effects of illumination intensity on bacteriochlorophyll *c* homolog distribution in *Chloroflexus aurantiacus* grown under controlled conditions. Photosynth Res 41:151–156

Ma YZ, Cox RP, Gillbro T, Miller M (1996) Bacteriochlorophyll organization and energy transfer kinetics in chlorosomes from *Chloroflexus aurantiacus* depend on the light regime during growth. Photosynth Res 47:157–165

Miyatake T, Tamiaki H (2005) Self-aggregates of bacteriochlorophylls-*c*, *d* and *e* in a light-harvesting antenna system of green photosynthetic bacteria: effect of stereochemistry at the chiral 3-(1-hydroxyethyl) group on the supramolecular arrangement of chlorophyllous pigments. J Photochem Photobiol C 6:89–107

Nozawa T, Ohtomo K, Suzuki M, Nakagawa H, Shikama Y, Konami H, Wang ZY (1994) Structures of chlorosomes and aggregated BChl *c* in *Chlorobium tepidum* from solid state high resolution CP/MAS ^{13}C NMR. Photosynth Res 41:211–223

Oostergetel GT, Reus M, Gomez Maqueo Chew A, Bryant DA, Boekema EJ, Holzwarth AR (2007) Long-range organization of bacteriochlorophyll in chlorosomes of *Chlorobium tepidum* investigated by cryo-electron microscopy. FEBS Lett 581: 5435–5439

Pedersen MO, Underhaug J, Dittmer J, Miller M, Nielsen NC (2008) The three-dimensional structure of CsmA: a small antenna protein from the green sulfur bacterium *Chlorobium tepidum*. FEBS Lett 582:2869–2874

Psencik J, Ma YZ, Arellano JB, Garcia-Gil J, Holzwarth AR, Gillbro T (2002) Excitation energy transfer in chlorosomes of *Chlorobium phaeobacteroides* strain CL1401: the role of carotenoids. Photosynth Res 71:5–18

Psencik J, Ikonen TP, Laurinmäki P, Merckel MC, Butcher SJ, Serimaa RE, Tuma R (2004) Lamellar organization of pigments in chlorosomes, the light harvesting complexes of green photosynthetic bacteria. Biophys J 87:1165–1172

Psencik J, Arellano JB, Ikonen TP, Borrego CM, Laurinmaki PA, Butcher SJ, Serimaa RE, Tuma R (2006) Internal structure of chlorosomes from brown-colored *Chlorobium* species and the role of carotenoids in their assembly. Biophys J 91:1433–1440

Psencik J, Collins AM, Liljeroos L, Torkkeli M, Laurinmaki P, Ansink HM, Ikonen TP, Serimaa RE, Blankenship RE, Tuma R, Butcher SJ (2009) Structure of chlorosomes from the green filamentous bacterium *Chloroflexus aurantiacus*. J Bacteriol 191:6701–6708

Schmidt K, Maarzahl M, Mayer F (1980) Development and pigmentation of chlorosomes in *Chloroflexus aurantiacus* strain Ok-70-fl. Arch Microbiol 127:87–97

Smith KM, Kehres LA, Fajer J (1983) Aggregation of the bacteriochlorophylls *c*, *d* and *e*. Models for the antenna chlorophylls of green and brown photosynthetic bacteria. J Am Chem Soc 105:1387–1389

Steensgaard DB, Wackerbarth H, Hildebrandt P, Holzwarth AR (2000) Diastereoselective control of bacteriochlorophyll *e* aggregation. 3(1)-S-BChl *e* is essential for the formation of chlorosome-like aggregates. J Phys Chem B 104:10379–10386

Umetsu M, Wang ZY, Zhang J, Ishii T, Uehara K, Inoko Y, Kobayashi M, Nozawa T (1999) How the formation process influences the structure of BChl c aggregates. Photosynth Res 60:229–239

van Rossum BJ, Boender GJ, Mulder FM, Raap J, Balaban TS, Holzwarth AR, Schaffner K, Prytulla S, Oschkinat H, de Groot HJM (1998) Multidimensional CP-MAS C-13 NMR of uniformly enriched chlorophyll. Spectrochim Acta A Mol Biol Spectrosc 54:1167–1176

Vassilieva EV, Stirewalt VL, Jakobs CU, Frigaard NU, Inoue-Sakamoto K, Baker MA, Sotak A, Bryant DA (2002) Subcellular localization of chlorosome proteins in *Chlorobium tepidum* and characterization of three new chlorosome proteins: CsmF, CsrnH, and CsmX. Biochemistry 41:4358–4370

Vila X, Abella CA (1994) Effects of light quality on the physiology and the ecology of planktonic green sulfur bacteria in lakes. Photosynth Res 41:53–65

Wahlund TM, Woese CR, Castenholz RW, Madigan MT (1991) A thermophilic green sulfur bacterium from New Zealand hot-springs, *Chlorobium tepidum* sp. nov. Arch Microbiol 156:81–90

Zupcanova A, Arellano JB, Bina D, Kopecky J, Psencik J, Vacha F (2008) The length of esterifying alcohol affects the aggregation properties of chlorosomal bacteriochlorophylls. Photochem Photobiol 84:1187–1194